

Analysis of Two Plane Electromechanical Model of Shape Deviation in a Hydropower Generator

PETER KIHLANGI

MASTER OF SCIENCE PROGRAMME
Mechanical Engineering

Luleå University of Technology
Department of Applied Physics and Mechanical Engineering
Division of Solid Mechanics



Analysis of Two Plane Electromechanical Model of Shape Deviation in a Hydropower Generator

Peter Kihlangi
Division of Computer Aided Design
Department of Applied Physics and Mechanical Engineering
Luleå University of Technology

April 2, 2007

Acknowledgement

This work has been carried out at Division of Computer Aided Design at Luleå University of Technology during the period 2006-2007 and is part of the ELEKTRA-project "*Methodlogy for characterizing modelling, and experimental verification of old in service hydropower units.*" . I want to thank my academic advisor Martin Karlsson and my examiner Jan-Olov Aidanpää for their engagement, support, discussion and review of my work.

I also want to thank my family and friends for their love and support.

This research was funded by Skellefteåkraft AB and I want to thank them for giving me the opportunity to work in this interesting field.

Abstract

Hydroelectric power supplies about 20 percent of the world's electricity and is the most important renewable energy converting industry. Swedish hydropower plants produce between 55-74TWh a year. These plants were built thirty to one hundred years ago and were constructed for base load. With new developments in energy production, for instance nuclear and renewable power, many hydropower plants have a new task, namely to function as regulators and keep frequency in the power net constant. Which means that constructions that were not built for it will have to do many starts and stops in their lifetime. This makes it interesting to examine the rotordynamic effects in hydropower generators.

All generators have shape deviations since it is not possible to manufacture perfect circular generators. Especially in Hydropower applications, where the diameter is normally large and the relative airgap is small. These properties make it likely that the response of the system depends on the shape deviation.

This thesis examines the effect shape deviation of the generator has on the response. It compares the difference between using the mean shape deviation on rotor and stator compared to two shape deviation one on the upper half of the rotor and stator and one the lower half. With two shape deviations there will be a bending moment due to the differences in shape of the upper and lower parts of the generator. The main goal is to investigate the effects of these bending moments and also to use a real generator as a model(Krångfors G2 at River Skellefte älv).

The results show that two shape deviations give rise to bending moments in new frequencies. There is only a very small effect on displacement response of the rotor. The new moments are seen in the angular response, where there is a clear difference between the two cases. In the case of Krångfors G2 it was found that the stiffness of the rotor was high and therefore only the first frequency of the shape deviations is likely affect the system. But, in other hydropower generators it is possible that the bending moments can affect the dynamics of the system. Then the methods presented in this thesis can be a valuable tool.

Contents

1	Introduction	11
1.1	Hydropower	11
1.2	Rotordynamics	12
1.3	Unbalanced Magnetic Pull	12
2	Modelling	13
2.1	Mechanical Model	13
2.1.1	The Gyroscopic Matrix	14
2.1.2	The Stiffness Matrix	15
2.1.3	The Damping Matrix	16
2.1.4	Unbalance	16
2.1.5	The Mechanical System	17
2.2	Magnetic Forces and Moments	17
2.2.1	Magnetic Forces	18
2.2.2	Magnetic Stiffness Matrix	18
2.2.3	Magnetic Forces due to Shape Deviation	20
2.3	Fourier Analysis of the Forces due to Shape Deviation	21
2.4	The Force Vectors due to Shape Deviation	22
3	Analysis	27
3.1	The State Vector Approach	27
3.2	Harmonic Excitation	28
4	Results	31
4.1	Magnetic Forces	31
4.2	Response	32
4.3	Response to special case	36
5	Discussion	39
5.1	Conclusions	40

Nomenclature

E	Young modulus	2.0e11 Pa
m_r	Mass rotor	98165 kg
m_p	Mass rotor poles	0 kg
α	Coefficient, length	-
β	Coefficient, length	-
J_d	Diametrical moment of inertia	226380 kgm ³
J_p	Polar moment of inertia	430000 kgm ³
L	Length of shaft	4.7 m
h	Height rotor poles	1.18
I	Moment of inertia shaft	0.0045
k_a	Stiffness bearing A	165e6 N/m
k_b	Stiffness bearing B	165e6 N/m
w_{dr}	Operating frequency	14.28 rad/s
c_a	Damping bearing A	230e3 kg/s
c_b	Damping bearing B	230e3 kg/s
l	Displacement rotorpoles	0 m
u	Position unbalance	4.44E-4
l_s	Position of shape deviation	0.3933 m
g_0	Average air-gap	0.0125 m
r_{rotor}	Rotor radius	2.7625 m
r_{stator}	Stator radius	2.7750 m

Chapter 1

Introduction

The global energy consumption is expected to increase from 111,000 TWH/year in 1997 to 178,000 TWH/year in 2020, this corresponds to a increase of 60%. The electric share of total energy consumption is expected to increase with 76% in the same time. This means that the global electricity production must increase [1]. Today Sweden produces 150TWh electricity a year and hydropower provides 55-75TWh of that, depending on the yearly rainfall. The electricity production from hydropower plants in Sweden is divided between ca 700 larger hydropower plants with effect of 1.5MW or more and 1200 smaller hydropower plants with an effect of 1.5MW or less [2]. The world's total estimated hydropower potential is 14370 TWH/year, of which about 8082 TWH/year is economically feasible to be developed. 700 GW (2600 TWH/year) is currently operating and 108 GW is under construction. Today hydropower produces about 20% of the world's electricity. China, India, Iran and Turkey have large-scale hydropower development programmes and there are projects that are under construction in about 80 countries. Many countries see hydropower as the key future electricity source, for example Sudan, Rwanda, Guinea, Cambodia, Cuba, Costa Rica and Guyana [1]. In Sweden it is possible expand the hydropower with 24TWh, but the Swedish, Parliament, Riksdagen has decided on a cap of 2TWh [2].

In Sweden the hydropower was built thirty to one hundred years ago and served as the base load deliverer. There is no way to store electric power in the form of electricity, therefore the electric power produced in power plants is the same as the power consumed. A over or under production of electricity will have effect on the frequency in the power net, because of this there has to be a way to regulate the production of electricity. Today many hydropower plants are frequently used to regulate the power production to keep the frequency in the power net at optimal frequency(49.9-50.1 Hz). Hydropower regulates also the long term power production that changes during the year.

1.1 Hydropower

A hydropower plant converts potential energy in water to electric energy in the power net. The water is lead to the turbine water via water ways. The turbine is connected to a generator by a shaft, when the turbine is set into motion by the

flowing water the generator will convert energy of motion into electric energy [2].

1.2 Rotordynamics

The research in the field of rotordynamics started with Rankine's [3] analysis of a spinning shaft in 1869, he used a faulty model and predicted incorrectly that a rotating machine could never operate above its first critical speed. Jeffcott [4] published in 1919 a new rotor model and derived a theory that shows that it's possible for a rotating machine to operate above its critical speeds. The influence of gyroscopic effects was presented by Stodola In 1924 [5]. Green [6] continued the work on gyroscopic effects 1948 with a four degree of freedom overhung rotor. Rotordynamics is considered a separate area within structural dynamics. The major differences from structural dynamics are that the eigenfrequencies are depended on the whirling speed due to the gyroscopic effect and that the directions of the vibrations are important in order to determine forward and backward whirl. For theory about rotordynamics, see for example the book by Yamamoto and Ishida [7]

1.3 Unbalanced Magnetic Pull

Gray et. al [8] critically reviews the bibliography on unbalanced magnetic pull (UMP) in dynamoelectric machines, among the reviews was the work of Behrend in which he suggested a linear equation for the UMP. Belmans et. al. [9] published a analytical model for vibrations due to eccentricity in induction motors. Arkkio et. al. [10] derived the electromagnetic force on a whirling cage rotor numerically with the use of finite element method (FEM) and showed that a simple force model can be used for rotordynamic calculations. Guo et. al. [11] published a analytical model of the UMP in a three-phase electric machine with any pole-pairs caused by a static and dynamic eccentricity. Wang et. al. [12] derived the UMP due to eccentricity through the law of energy conservation and studied the free and forced vibrations for rotors of electric motors. Gustavsson et. al. [13] published a linear model for radial magnetic pull in a synchronous hydropower generator and used it to analyze the motion of a hydropower rotor due to static and dynamic eccentricity. Karlsson et. al. [14] analyzed the effect of a shape deviation in a hydropower generator, and how it effected the forces on the rotor due to the magnetic field between the rotor and stator. Lundstrom et. al. [15] published a analytical model for an arbitrary shape deviation in a hydropower generator. Lundstrom et. al. [16] showed that there exist a tangential magnetic force component in synchronous machines due to the damping winding and used a linearised model to analyze the rotor dynamical behavior of these forces. This thesis continues the work of Karlsson by expanding the problem to two shape deviations, one on the upper half of the rotor and stator and one on the lower half.

Chapter 2

Modelling

2.1 Mechanical Model

In this report the model for a hydropower rotor system, consists of a flexible mass less shaft of the length L , area moment of inertia I and Young's modulus E . The shaft is supported by two bearings with stiffness k_a and k_b and damping c_a and c_b . The position of the rotor from the top bearing is set by α and the position of the rotor from the bottom bearing is β . The rotor is modelled as a disc, with mass m_r diametrical moment of inertia J_d , polar moment of inertia J_p , displacement of rotor poles in the Z-direction l (the rotor poles are modelled as a circular ring around the rotor and they can be displaced, which gives a displacement of the center of mass) and h the height of the rotor poles, with a circular ring around it corresponding to the rotor poles with mass m_p , see Figure 2.1.

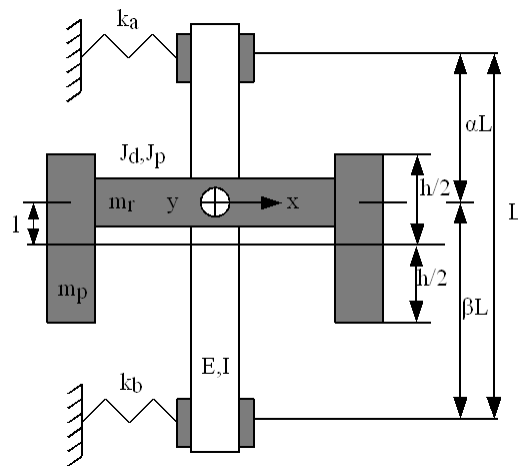


Figure 2.1: Rotor geometry.

The disc can translate in the x and y direction and rotate around the same axes, this gives the model four degrees of freedom. Lagrange's Equation is used to the equations of motion, these can with matrix notation be written as:

$$\overline{M} \ddot{\vec{x}} + (\omega \overline{G} + \overline{C}) \dot{\vec{x}} + (\overline{K} - \overline{K}_m) \vec{x} = \overline{F}_{unbalance} + \overline{F}_{shape}. \quad (2.1)$$

Where \overline{M} is the diagonal mass matrix where the entry's are the total mass of the rotor $m = m_r + m_p$, (where m_r is the mass of the rotor and m_p is the mass of the rotor poles) and the total diametrical moment of inertia $J = J_d + m_p l^2$ of the rotor (where J_d is the diametric moment of inertia for the rotor and $m_p l^2$ is an extra term due to displacement of the center of mass [17]), w is the driving frequency, \overline{G} is the gyroscopic matrix, \overline{K} is the stiffness matrix, \overline{K}_m is the magnetic stiffness matrix, $\overline{F}_{unbalance}$ is the force due to unbalance and \overline{F}_{shape} is the force due to shape deviation of rotor and stator.

2.1.1 The Gyroscopic Matrix

If the disc in the model has an inclination vibration θ_x, θ_y , it will result in an effect that is called a gyroscopic moment. The disc has a polar moment of inertia J_p , but the angular velocity vector $\vec{\omega}t$ of the disc no longer points in the z-axis direction, a transformation of the rotation vector is needed to be able to describe the rotation in the xyz frame, this is carried out by *Genta* [18] and the result can be summarized in the gyroscopic matrix:

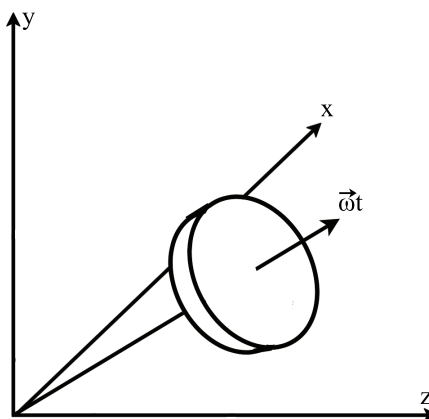


Figure 2.2: Disc in z-x/y plane, the angular velocity vector $\vec{\omega}t$.

$$\begin{pmatrix} 0 & 0 & 0 & 0 \\ 0 & 0 & 0 & 0 \\ 0 & 0 & 0 & wJ_p \\ 0 & 0 & -wJ_p & 0 \end{pmatrix}. \quad (2.2)$$

2.1.2 The Stiffness Matrix

The stiffness matrix is derived from the relation between the displacement of the system and the forces acting on it. When deriving the stiffness matrix it is easier to calculate its inverse which is called the flexibility matrix A [17]:

$$\overline{K}\overline{x} = \overline{P} \Leftrightarrow \overline{x} = \overline{K}^{-1}\overline{P} = \overline{AP}. \quad (2.3)$$

The flexibility matrix A is derived using beam theory and the stiffness from the bearings [17]:

$$\begin{pmatrix} y \\ x \\ \theta_y \\ \theta_x \end{pmatrix} = \begin{pmatrix} \alpha_1 & 0 & 0 & -\alpha_2 \\ 0 & \alpha_1 & \alpha_2 & 0 \\ 0 & \alpha_2 & \alpha_3 & 0 \\ -\alpha_2 & 0 & 0 & \alpha_3 \end{pmatrix} \begin{pmatrix} P_y \\ P_x \\ M_y \\ M_x \end{pmatrix}, \quad (2.4)$$

$$\alpha_1 = \frac{L^3\alpha^2\beta^2}{3EI} + \left(\frac{\alpha^2}{k_b} + \frac{\beta^2}{k_a} \right), \quad (2.5)$$

$$\alpha_2 = \frac{L^2\alpha\beta(\alpha - \beta)}{3EI} - \frac{1}{L} \left(\frac{\alpha}{k_b} - \frac{\beta}{k_a} \right), \quad (2.6)$$

$$\alpha_3 = \frac{L(1 - 3\alpha\beta)}{3EI} + \frac{1}{L} \left(\frac{1}{k_b} + \frac{1}{k_a} \right) \quad (2.7)$$

and

$$\beta = \alpha - 1. \quad (2.8)$$

Where L is the length of the shaft, E is the Young's modulus, I the area moments of inertia, k_a stiffness for bearing a and k_b stiffness for bearing b. The first part in Equation (2.5), (2.6) and (2.7) is the stiffness in the shaft, the second part is due to the stiffness in the bearings. Using Equation (2.3) the stiffness matrix is:

$$\begin{pmatrix} P_y \\ P_x \\ M_y \\ M_x \end{pmatrix} = \begin{pmatrix} k_1 & 0 & 0 & k_2 \\ 0 & k_1 & -k_2 & 0 \\ 0 & -k_2 & k_3 & 0 \\ k_2 & 0 & 0 & k_3 \end{pmatrix} \begin{pmatrix} y \\ x \\ \theta_y \\ \theta_x \end{pmatrix}. \quad (2.9)$$

2.1.3 The Damping Matrix

The damping matrix is derived in the same manner as the bearing part of the stiffness matrix, except that k_a and k_b are replaced with c_a and c_b . This results in the damping correspondence to the flexibility matrix:

$$\begin{pmatrix} A_1 & 0 & 0 & -A_2 \\ 0 & A_1 & A_2 & 0 \\ 0 & A_2 & A_3 & 0 \\ -A_2 & 0 & 0 & A_3 \end{pmatrix}, \quad (2.10)$$

where

$$A_1 = \frac{\alpha^2}{c_b} + \frac{\beta^2}{c_a}, \quad (2.11)$$

$$A_2 = -\frac{1}{L} \left(\frac{\alpha}{c_b} - \frac{\beta}{c_a} \right) \quad (2.12)$$

and

$$A_3 = \frac{1}{L} \left(\frac{1}{c_b} + \frac{1}{c_a} \right). \quad (2.13)$$

The inverse gives the damping matrix:

$$\begin{pmatrix} c_1 & 0 & 0 & c_2 \\ 0 & c_1 & -c_2 & 0 \\ 0 & -c_2 & c_3 & 0 \\ c_2 & 0 & 0 & c_3 \end{pmatrix}. \quad (2.14)$$

2.1.4 Unbalance

In a real generator there will always exist an unbalance. Unbalance is a small displacement of the center of mass of the rotor P compared to the geometrical center of the rotor C see Figure 2.3. The unbalance can be modulated as a harmonic excitation of the system:

$$F_{unbalance} = \begin{pmatrix} m\omega^2 u \cos(\omega t) \\ m\omega^2 u \sin(\omega t) \\ 0 \\ 0 \end{pmatrix}. \quad (2.15)$$

Where m is the mass of the rotor, ω the rotation frequency of the rotor and u the distance from the geometrical center to the center of mass of the rotor.

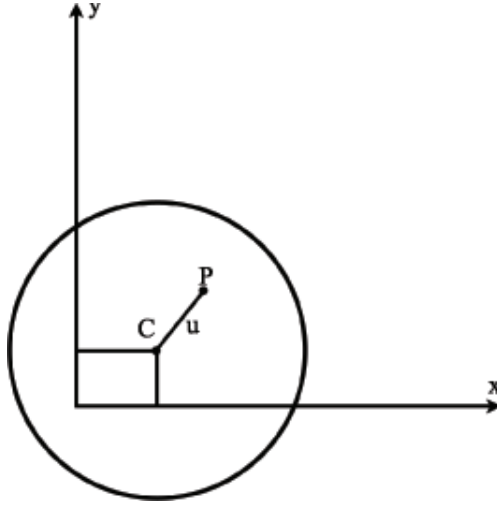


Figure 2.3: P is the center of mass (position of unbalance), C is the geometrical center and u is the distance from C to P .

2.1.5 The Mechanical System

The system can now be written in matrix form as:

$$\begin{aligned}
 & \begin{pmatrix} m_r + m_p & 0 & 0 & 0 \\ 0 & m_r + m_p & 0 & 0 \\ 0 & 0 & J_d + m_p l^2 & 0 \\ 0 & 0 & 0 & J_d + m_p l^2 \end{pmatrix} \begin{pmatrix} \ddot{x} \\ \ddot{y} \\ \ddot{\theta}_x \\ \ddot{\theta}_y \end{pmatrix} + \\
 & \left(\begin{pmatrix} 0 & 0 & 0 & 0 \\ 0 & 0 & 0 & 0 \\ 0 & 0 & 0 & \omega J_p \\ 0 & 0 & -\omega J_p & 0 \end{pmatrix} + \begin{pmatrix} c_1 & 0 & 0 & c_2 \\ 0 & c_1 & -c_2 & 0 \\ 0 & -c_2 & c_3 & 0 \\ c_2 & 0 & 0 & c_3 \end{pmatrix} \right) \begin{pmatrix} \dot{x} \\ \dot{y} \\ \dot{\theta}_x \\ \dot{\theta}_y \end{pmatrix} + \quad (2.16) \\
 & \begin{pmatrix} k_1 & 0 & 0 & k_2 \\ 0 & k_1 & -k_2 & 0 \\ 0 & -k_2 & k_3 & 0 \\ k_2 & 0 & 0 & k_3 \end{pmatrix} \begin{pmatrix} x \\ y \\ \theta_x \\ \theta_y \end{pmatrix} = \begin{pmatrix} m\omega^2 u \cos(\omega t) \\ m\omega^2 u \sin(\omega t) \\ 0 \\ 0 \end{pmatrix}.
 \end{aligned}$$

2.2 Magnetic Forces and Moments

In a completely symmetric generator all magnetic moments and forces would cancel, in reality this is never the case since there will always exist some form of asymmetry. The asymmetry is usually divided into eccentricity and shape deviation see Figure 2.4 and 2.8. It has been shown [13] that the magnetic forces must be taken in account when calculating on the stability of a generator.

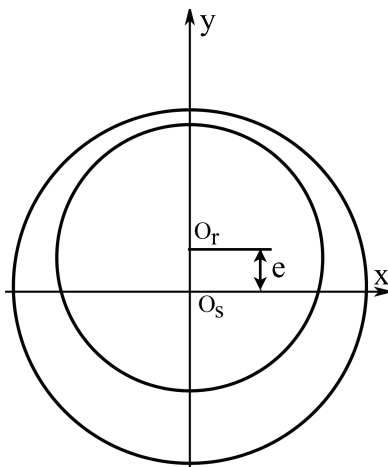


Figure 2.4: A rotor with eccentricity, e , in the y -direction inside the stator. O_r and O_s denotes the origin of the rotor and the stator.

2.2.1 Magnetic Forces

Wang et. al. [12] shows that for an symmetric circular rotor and stator the force due to displacement of the rotor the magnetic force in the x -direction is (the force in y -direction is derived in a similar way):

$$f_x = k_m \frac{x}{\left(1 - \frac{x^2}{g_0^2}\right)^{3/2}}. \quad (2.17)$$

Where k_m is called the magnetic stiffness and is dependent on the height of the generator, permeability of air, mean radius of the rotor and stator, average air-gap g_0 and the magnetic-flux density.

In this thesis the value for k_m is a approximate value given by the manufacturer of the generator, so no calculations of k_m is necessary. The force f_x is still non-linear, but in this thesis only small perturbation are considered, $x \ll g_0$. Figure 2.5 . Equation (2.17) can therefore be rewritten as:

$$f_x = k_x x. \quad (2.18)$$

Which is a linear equation for the magnetic force and also gives the forces due to displacement of the rotor.

2.2.2 Magnetic Stiffness Matrix

Eccentric and angular displacement will cause a disturbance in the magnetic field, which will result in a magnetic force and moment on the rotor. For rotor displacement up to 10% the magnetic forces can be linearised, see Figure 2.5. Equation 2.18 gives the magnetic forces due to displacement in the x and y

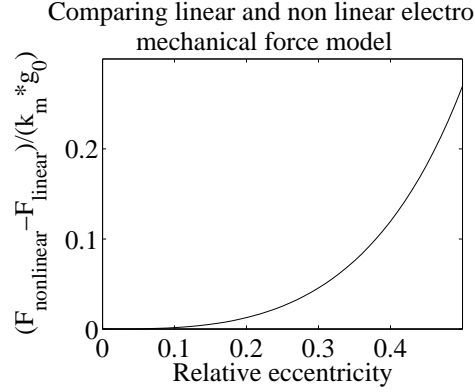


Figure 2.5: Error of the non-linear approximation to the electro-mechanical force due to eccentricity.

direction. The forces due to angular displacement and displacement are given by [13] (the second term is the force due to angular displacement):

$$F_x = \frac{k_m \delta_x}{h} \int_{-(\frac{h}{2}-l)}^{\frac{h}{2}+l} d\xi + \frac{k_m \theta_y}{h} \int_{-(\frac{h}{2}-l)}^{\frac{h}{2}+l} \xi d\xi = k_m \delta_x + k_m \theta_y l \quad (2.19)$$

and

$$F_y = \frac{k_m \delta_y}{h} \int_{-(\frac{h}{2}-l)}^{\frac{h}{2}+l} d\xi - \frac{k_m \theta_x}{h} \int_{-(\frac{h}{2}-l)}^{\frac{h}{2}+l} \xi d\xi = k_m \delta_y - k_m \theta_x l. \quad (2.20)$$

When calculating the moments due to displacement and angular displacement, the forces in Equation (2.19) and (2.20) are multiplied with the corresponding lever, this gives:

$$M_x = -\frac{k_m \delta_y}{h} \int_{-(\frac{h}{2}-l)}^{\frac{h}{2}+l} \xi d\xi + \frac{k_m \theta_x}{h} \int_{-(\frac{h}{2}-l)}^{\frac{h}{2}+l} \xi^2 d\xi = -k_m l \delta_x + \frac{k_m \theta_x}{3h} \left[\left(\frac{h}{2} + l\right)^3 + \left(\frac{h}{2} - l\right)^3 \right] \quad (2.21)$$

and

$$M_y = \frac{k_m \delta_x}{h} \int_{-(\frac{h}{2}-l)}^{\frac{h}{2}+l} \xi d\xi + \frac{k_m \theta_y}{h} \int_{-(\frac{h}{2}-l)}^{\frac{h}{2}+l} \xi^2 d\xi = k_m l \delta_x + \frac{k_m \theta_y}{3h} \left[\left(\frac{h}{2} + l\right)^3 + \left(\frac{h}{2} - l\right)^3 \right]. \quad (2.22)$$

Equation (2.19), (2.20), (2.21) and (2.22) can be written as the magnetic stiffness matrix K_m [13]:

$$\vec{F} = \overline{K}_m \vec{x} \quad (2.23)$$

where \overline{K}_m is

$$k_m \begin{pmatrix} 1 & 0 & 0 & l \\ 0 & 1 & -l & 0 \\ 0 & -l & \Gamma & 0 \\ l & 0 & 0 & \Gamma \end{pmatrix} \quad (2.24)$$

and Γ is defined as

$$\Gamma = \frac{1}{3h} \left[\left(\frac{h}{2} + l \right)^3 + \left(\frac{h}{2} - l \right)^3 \right]. \quad (2.25)$$

This is the magnetic stiffness matrix and it describes the forces due to angular displacement and displacement of a perfect circular rotor and stator, with no shape deviation.

2.2.3 Magnetic Forces due to Shape Deviation

To derive the shape deviations, it is preferred to assume a centered symmetric rotor. Now it's possible to derive the shape deviations as the difference in the air gap to the symmetric rotor air gap also called the nominal air gap, this difference can be described by [14]:

$$\Delta_{gap}(i, j) = \Delta_r(i, j) - \Delta_s(i, j). \quad (2.26)$$

The rotor is described by a number of discrete gaps, describing the gaps between the rotor poles and the stator. Where $\Delta_r(i, j)$ is the difference to nominal rotor radius, $\Delta_s(i, j)$ is the difference to nominal stator radius, i is the index of the rotor pole and j is the order of rotor rotation. Angle between each pole is described by [14]:

$$\psi = \frac{1}{n} 2\pi. \quad (2.27)$$

Where n is the number of discrete gaps. To get the total force acting on the rotor due to the shape deviation, all the forces must be summarized around the whole rotor. The magnetic stiffness for the whole rotor is given by k_m which is a measured constant. To derive the total force, $k_{m,i}$ for each rotor pole is needed. The displacement from nominal air gap at a discrete gap is given by:

$$\Delta X \cos(\psi_i). \quad (2.28)$$

The force in x-direction from one rotor pole is given by:

$$F_{x_i} = (k_{m,i} \Delta X \cos(\psi_i)) \cos(\psi_i). \quad (2.29)$$

The total force in x-direction is given by:

$$k_m \Delta X = \sum k_{m,i} \Delta X \cos(\psi_i)^2 = k_{m,i} \Delta X \sum \left(\frac{1}{2} + \frac{\cos(2\psi_i)}{2} \right), \quad (2.30)$$

but

$$\sum \frac{\cos(2\psi_i)}{2} = 0. \quad (2.31)$$

Since ψ goes from zero to 2π . This gives that:

$$k_{m,i} = \frac{2k_m}{n}, \quad (2.32)$$

for all i . By using simple geometry the total force in the x and y direction are [14]:

$$F_x(j) = \sum_{i=1}^n \Delta_{gap}(i, j) \cos\left((i-1)\frac{1}{n}2\pi\right) \frac{2k_{m,r}}{n} \quad (2.33)$$

and

$$F_y(j) = \sum_{i=1}^n \Delta_{gap}(i, j) \sin\left((i-1)\frac{1}{n}2\pi\right) \frac{2k_{m,r}}{n}. \quad (2.34)$$

2.3 Fourier Analysis of the Forces due to Shape Deviation

Fourier analysis is used to analyze the forces due to shape deviations, according to [7], the discrete Fourier transform is:

$$X(n) = \frac{1}{N} \sum_{k=0}^{N-1} x_k^{-i2\pi nk/N}. \quad (2.35)$$

The corresponding normalized frequency is calculated by:

$$f(n) = \frac{1}{dt} \frac{n}{N} \frac{2\pi}{w_{dr}}. \quad (2.36)$$

Where dt is the discrete time step, n the current number of steps, N the total number of steps, w_{dr} the driving frequency of the rotor. By analyzing the forces due to shape deviation in x and y-direction, it is found that there exists only frequencies that are multiples of the driving frequency, the 36 first frequencies are used to reconstruct the forces due to shape deviation by a sum of harmonic forces:

$$F(t) = \sum_{i=1}^n (A_i \sin(w_i t) + B_i \cos(w_i t)). \quad (2.37)$$

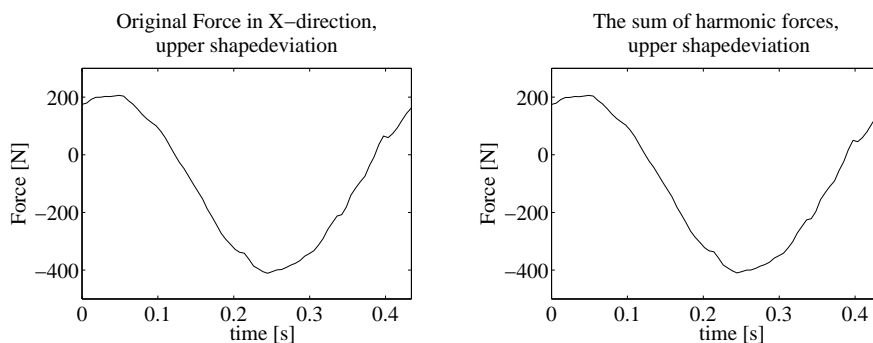


Figure 2.6: Force in the x-direction, from the upper shape deviation. (Left) the original force computed from measurements. (Right) Sum of harmonic according to Equation (2.37).

2.4 The Force Vectors due to Shape Deviation

By using the sum of harmonic forces in Equation (2.37) to describe the shape deviation, only the amplitudes, phase and the frequency of the forces are needed to solve the response for the whole system. Three cases of forces will be studied:

- Forces due to mean shape deviation. The mean force is calculated from two measured shape deviations.
- Forces and moments due to two shape deviations. The two measured shape deviations are used to calculate forces and moments.
- Forces and moments due to mean shape deviation only on the upper part of the generator. Special case: corresponds theoretically to a asymmetric rotor, with large shape deviation on the upper part.

For the case with one shape deviation for the whole rotor it is easy, the shape deviation will affect the system in the same way as an unbalance in the rotor would. $A_{xu,i}$ is the x-amplitude for sinus for the upper shape deviation, $A_{xl,i}$ is the x-amplitude for cosinus for the lower shape deviation and so forth:

$$\vec{A}_i = \begin{pmatrix} A_{xu,i} + A_{xl,i} \\ A_{yu,i} + A_{yl,i} \\ 0 \\ 0 \end{pmatrix} \quad (2.38)$$

and

$$\vec{B}_i = \begin{pmatrix} B_{xu,i} + B_{xl,i} \\ B_{yu,i} + B_{yl,i} \\ 0 \\ 0 \end{pmatrix}. \quad (2.39)$$

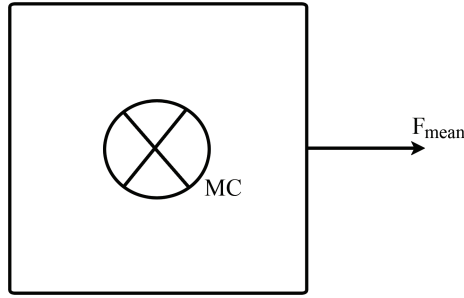


Figure 2.7: Force due to mean shape deviation.

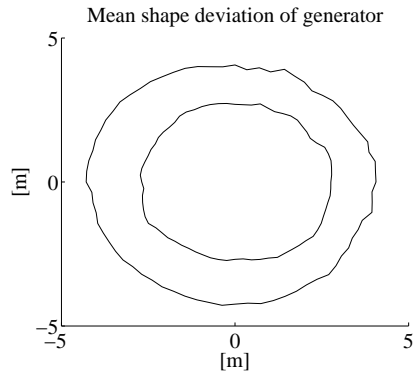


Figure 2.8: The mean shape deviation of the generator. The stator radius has been increased with 50% and the shape deviation with a factor 1000.

For two shape deviations, one on the upper half of the rotor and one on the lower half of the rotor, the vectors are derived by the use of simple mechanics with levering arms. Where l_s has the length $1/3h$ and is due to the bending moment:

$$\vec{A}_i = \begin{pmatrix} A_{xu,i} + A_{xl,i} \\ A_{yu,i} + A_{yl,i} \\ A_{yu,i} * l_s - A_{yl,i} * l_s \\ -A_{xu,i} * l_s + A_{xl,i} * l_s \end{pmatrix} \quad (2.40)$$

and

$$\vec{B}_i = \begin{pmatrix} B_{xu,i} + B_{xl,i} \\ B_{yu,i} + B_{yl,i} \\ B_{yu,i} * l_s - B_{yl,i} * l_s \\ -B_{xu,i} * l_s + B_{xl,i} * l_s \end{pmatrix}. \quad (2.41)$$

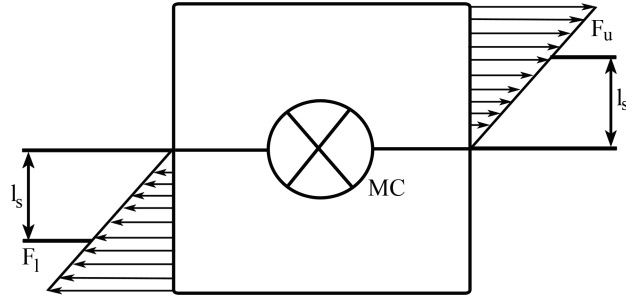


Figure 2.9: Force and moments due to two shape deviations.

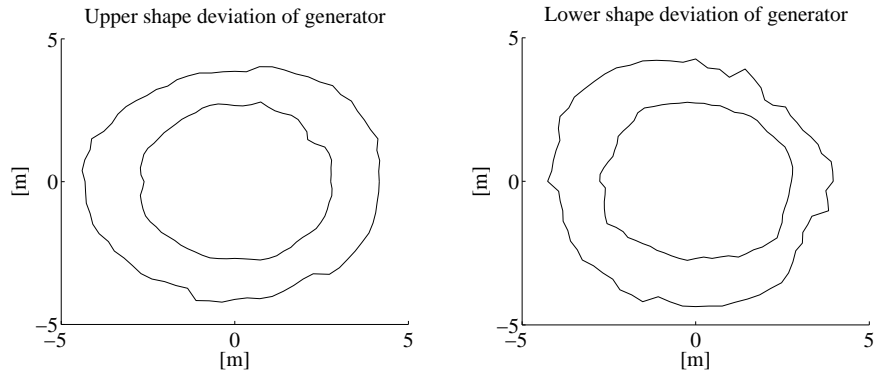


Figure 2.10: The two shape deviations of the generator. The stator radius has been increased with 50% and the shape deviation with a factor 1000.

For the mean shape deviation on the upper half of the rotor and no shape deviation on the lower, the vectors are derived in a similar way as for the case with two shape deviations. But now the moments will work in the same direction:

$$\vec{A}_i = \begin{pmatrix} A_{xu,i} + A_{xl,i} \\ A_{yu,i} + A_{yl,i} \\ A_{yu,i} * l_s + A_{yl,i} * l_s \\ -A_{xu,i} * l_s - A_{xl,i} * l_s \end{pmatrix} \quad (2.42)$$

and

$$\vec{B}_i = \begin{pmatrix} B_{xu,i} + B_{xl,i} \\ B_{yu,i} + B_{yl,i} \\ B_{yu,i} * l_s + B_{yl,i} * l_s \\ -B_{xu,i} * l_s - B_{xl,i} * l_s \end{pmatrix}. \quad (2.43)$$

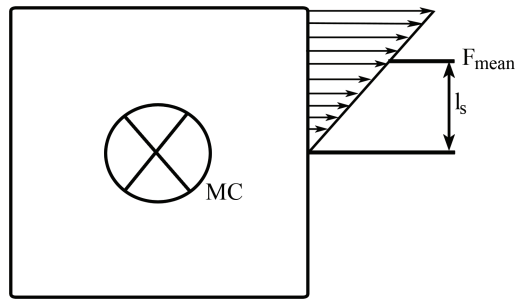


Figure 2.11: Mean shape deviation on the upper half of the generator, no shape deviation on the lower half.

The values for A and B are used to solve the response.

Chapter 3

Analysis

3.1 The State Vector Approach

To solve the system in this thesis, the state vector approach [19] is used. The system can be described by Equation (3.1):

$$\overline{M}\ddot{\vec{x}} + (\omega\overline{G} + \overline{C})\dot{\vec{x}} + (\overline{K} - \overline{K}_M)\vec{x} = \vec{F}_{umbalace} + \vec{F}_{shape}. \quad (3.1)$$

The first step in the state vector approach is to rewrite Equation (3.1) as a system of differential equations of the first degree:

$$\overline{y} = \begin{pmatrix} \overline{x} \\ \dot{\overline{x}} \end{pmatrix}. \quad (3.2)$$

Equation of motion now becomes:

$$\begin{pmatrix} -\overline{I} & \overline{N} \\ \overline{N} & \overline{M} \end{pmatrix} \begin{pmatrix} \overline{\dot{x}} \\ \overline{\ddot{x}} \end{pmatrix} + \begin{pmatrix} \overline{N} & \overline{I} \\ \overline{K} - \overline{K}_m & \omega\overline{G} \end{pmatrix} \begin{pmatrix} \overline{x} \\ \overline{\dot{x}} \end{pmatrix} = \begin{pmatrix} \overline{B} \\ \overline{F} \end{pmatrix}. \quad (3.3)$$

Where \overline{N} and \overline{B} are zero valued matrix respective vector. With matrix notation Equation (3.3) becomes:

$$-\overline{S}\overline{\dot{y}} + \overline{R}\overline{y} = \overline{H}. \quad (3.4)$$

To solve the homogenous solution for the system, it is assumed that H in Equation (3.4) is equal to a zero-vector. This corresponds to a system with no excitation. Then there exists a solution on the form $\overline{y} = \overline{DY}e^{\lambda t}$. Equation (3.4) becomes:

$$-\overline{S}\lambda\overline{DY}e^{\lambda t} + \overline{RDY}e^{\lambda t} = \overline{0}, \quad (3.5)$$

↓

$$(-\lambda\bar{S} + \bar{R})\bar{Y} = \bar{0}. \quad (3.6)$$

Simplifying by multiplying with \bar{S}^{-1} , gives Equation (3.7) where $\bar{A} = \bar{S}^{-1}\bar{R}$:

$$(\bar{A} - \lambda\bar{I})\bar{Y} = \bar{0}. \quad (3.7)$$

The solution to the homogenous part of the differential equation will be derived from the eigenvectors \bar{Y}_i and the eigenvalues λ_i , this gives a solution on the form:

$$\bar{Y}_h(t) = \sum_{i=1}^n D_i \bar{Y}_i e^{\lambda_i t}. \quad (3.8)$$

Which is the homogenous solution D_i is derived from the initial conditions. The eigenvalues are complex:

$$\lambda_i = \tau_i + iw_{d,i}. \quad (3.9)$$

Where τ_i is the decay rate and $w_{d,i}$ the damped eigenfrequency of the system. Of main interest in this thesis is the damped eigenfrequencies, which are used to see if any of the frequencies of the shape deviations might have large effects on the system.

3.2 Harmonic Excitation

If the system is excited by harmonic forces, the solution corresponds to the equation of motion when the homogenous solution has damped out. This is called the steady state solution and is also known as the particular solution. For harmonic excitations the forces in Equation (3.4) can be expressed as:

$$\bar{F}(t)_i = \bar{A}_i \sin(w_i t) + \bar{B}_i \cos(w_i t). \quad (3.10)$$

The particular solution is assumed to be:

$$\bar{y}(t)_{p,i} = \bar{a}_i \sin(w_i t) + \bar{b}_i \cos(w_i t). \quad (3.11)$$

By using Equation (3.11) in Equation (3.4) and solving for \bar{a}_i and \bar{b}_i the following equations are obtained:

$$\vec{a}_i = \left[w_i^2 \overline{SR}^{-1} \overline{S} + \overline{R} \right]^{-1} \left[\vec{A}_i - w_i \overline{SR}^{-1} \vec{B}_i \right] \quad (3.12)$$

and

$$\vec{b}_i = \overline{R}^{-1} \left[\vec{B}_i + w_i \overline{S} \vec{a}_i \right]. \quad (3.13)$$

Equation (3.12) and (3.13) will be used to solve the response from the unbalance and the shape deviation. The solution of the system will be the sum of the particular solutions:

$$\vec{Y}_p(t) = \sum_{i=1}^n \left(\vec{a}_i \sin(w_i t) + \vec{b}_i \cos(w_i t) \right). \quad (3.14)$$

Equation (3.14) is used to solve the response from harmonic excitations, in this case excitations from the shape deviations.

Chapter 4

Results

In this thesis, there is no displacement of the rotor poles ($l = 0$). The simulation of the response has been done for two cases of the placement of the rotor on the shaft, $\alpha = 0.50$ was chosen to see the effects of two shape deviation with no gyroscopic effects and $\alpha = 0.32$ is the α value of Krångfors G2. In Figure 4.1-4.14 max. amp. is the amplitude of the first frequency ($w/w_{dr} = 1$), the figures are zoomed up to visualize the other components.

4.1 Magnetic Forces

The frequency input of the magnetic forces and moments for the case of a mean shape deviation and for the case of two shape deviations where calculated with DFT.(Discrete Fourier Transform) plots of the frequencies found are seen in Figure 4.1 to 4.4.

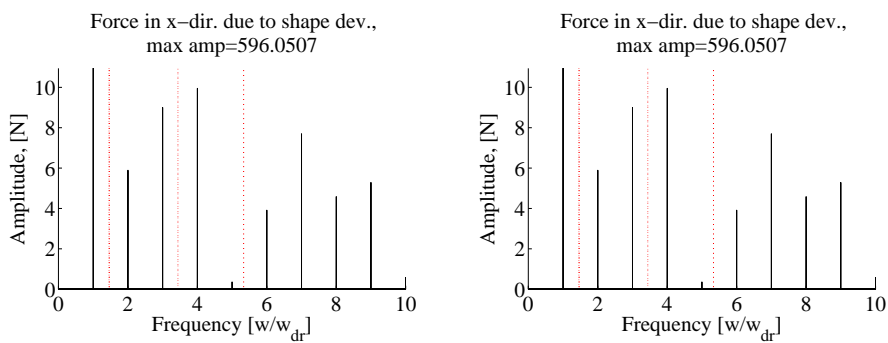


Figure 4.1: Force in the x-direction, black lines are the amplitudes of the forces in the simulation, red lines are the eigenfrequencies of the system. (Left) mean shape deviation. (Right) two shape deviations.

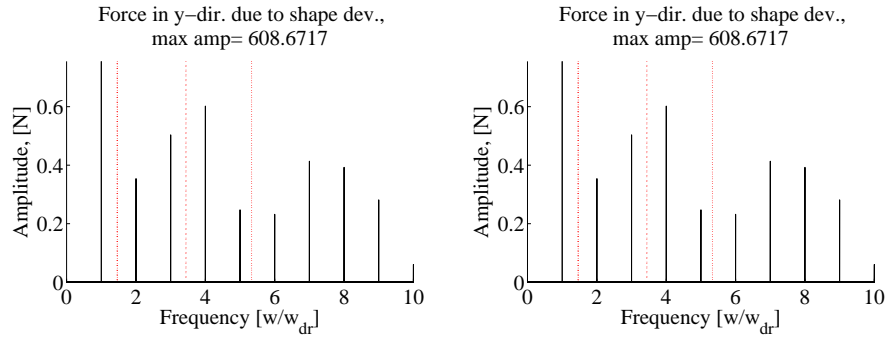


Figure 4.2: Force in the y-direction, black lines are the amplitudes of the forces in the simulation, red lines are the eigenfrequencies of the system. (Left) mean shape deviation. (Right) two shape deviations.

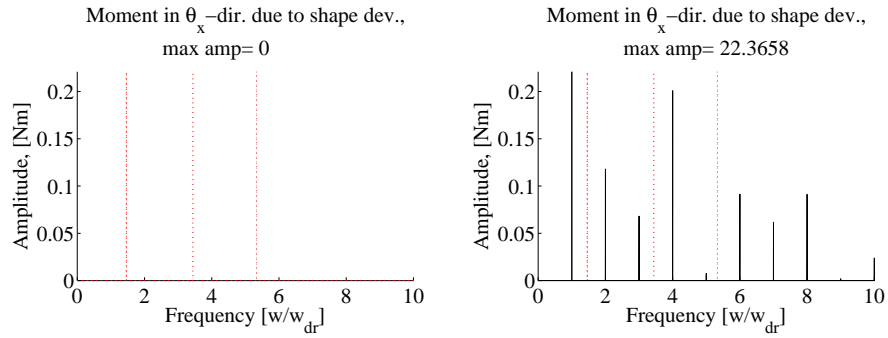


Figure 4.3: Bending moment in the θ_x direction, black lines are the amplitudes of the moments in the simulation, red lines are the eigenfrequencies of the system. (Left) mean shape deviation. (Right) two shape deviations.

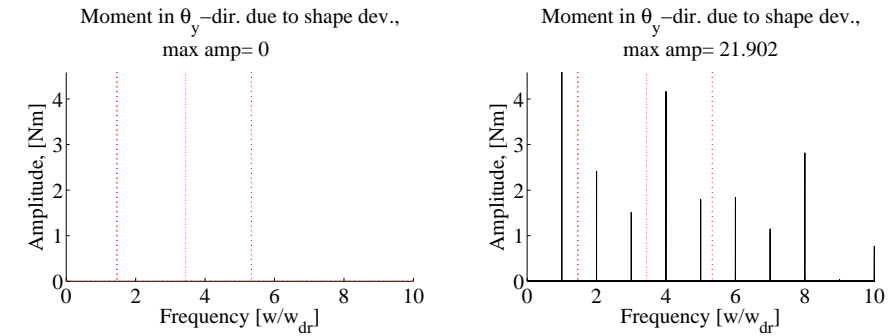


Figure 4.4: Bending moment in the θ_y direction, black lines are the amplitudes of the moments in the simulation, red lines are the eigenfrequencies of the system. (Left) mean shape deviation. (Right) two shape deviations.

4.2 Response

The response due to the magnetic force for the two cases, mean shape deviation and two shape deviations.

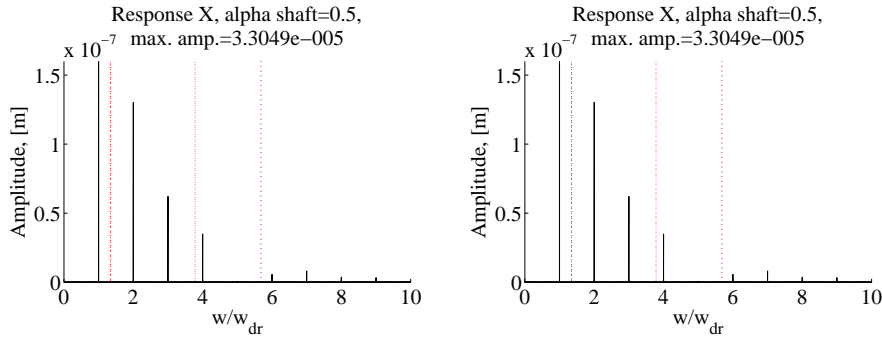


Figure 4.5: Response in X, $\alpha = 0.5$. Black lines are the amplitudes of the response in the simulation, red lines are the eigenfrequencies of the system. (Left) mean shape deviation. (Right) two shape deviations.

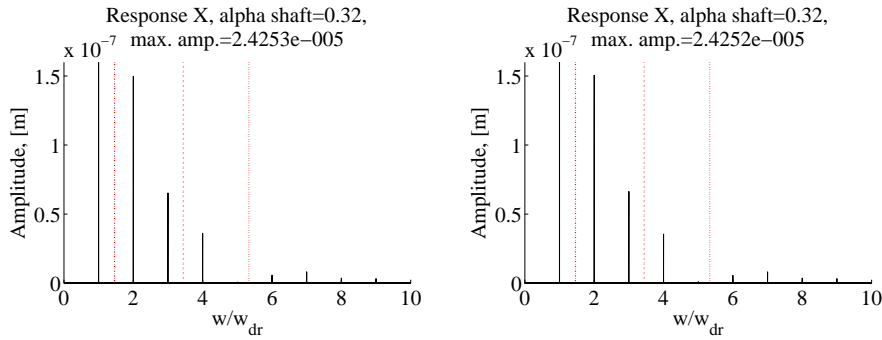


Figure 4.6: Response in X, $\alpha = 0.32$. Black lines are the amplitudes of the response in the simulation, red lines are the eigenfrequencies of the system. (Left) mean shape deviation. (Right) two shape deviations.

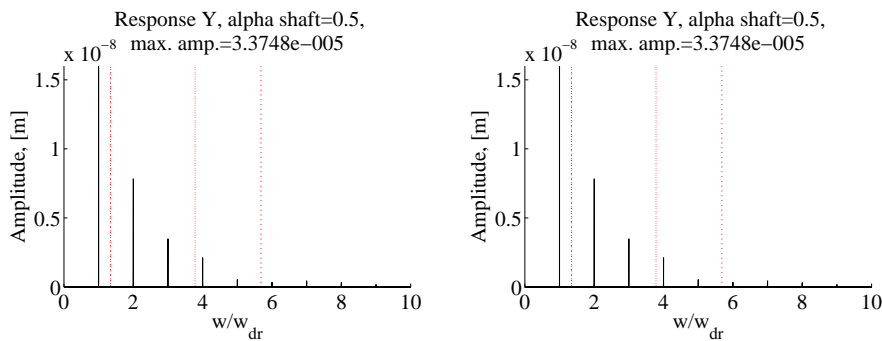


Figure 4.7: Response in Y, $\alpha = 0.5$. Black lines are the amplitudes of the response in the simulation, red lines are the eigenfrequencies of the system. (Left) mean shape deviation. (Right) two shape deviations.

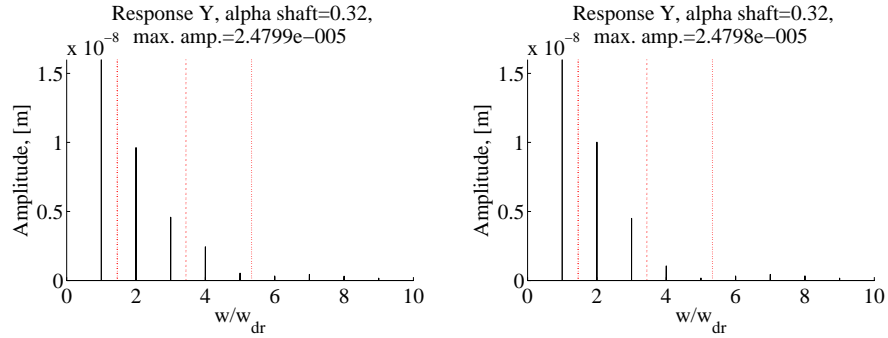


Figure 4.8: Response in Y , $\alpha = 0.32$. Black lines are the amplitudes of the response in the simulation, red lines are the eigenfrequencies of the system. (Left) mean shape deviation. (Right) two shape deviations.

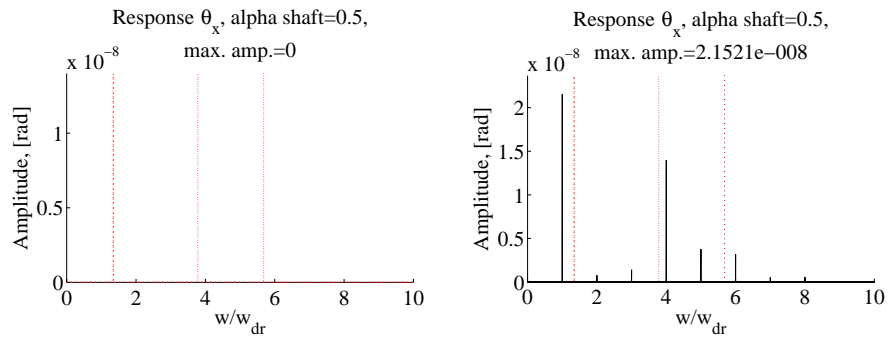


Figure 4.9: Response in θ_x , $\alpha = 0.5$. Black lines are the amplitudes of the response in the simulation, red lines are the eigenfrequencies of the system. (Left) mean shape deviation. (Right) two shape deviations.

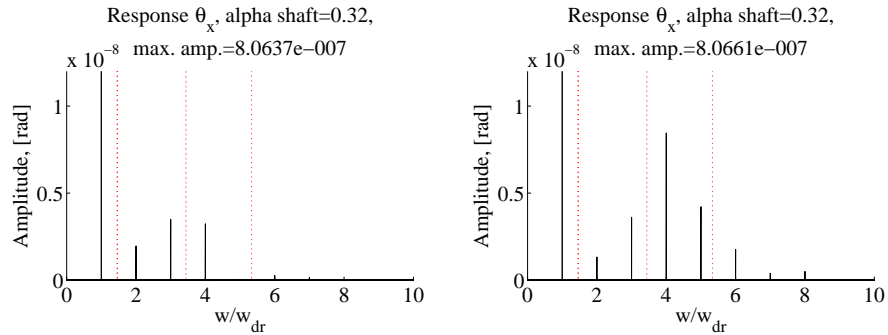


Figure 4.10: Response in θ_x , $\alpha = 0.32$. Black lines are the amplitudes of the response in the simulation, red lines are the eigenfrequencies of the system. (Left) mean shape deviation. (Right) two shape deviations.

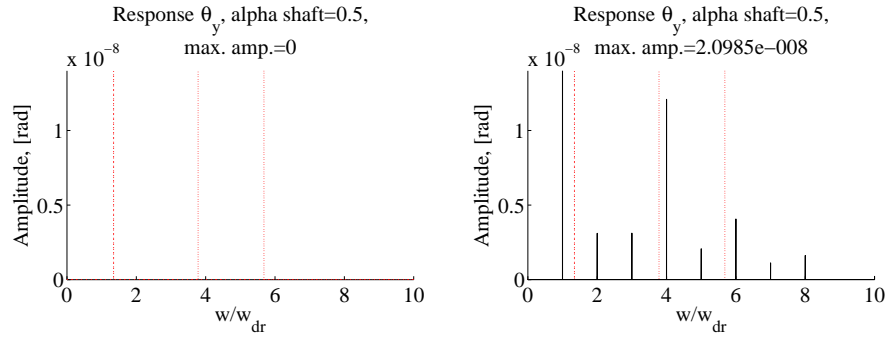


Figure 4.11: Response in θ_y , $\alpha = 0.5$. Black lines are the amplitudes of the response in the simulation, red lines are the eigenfrequencies of the system. (Left) mean shape deviation. (Right) two shape deviations.

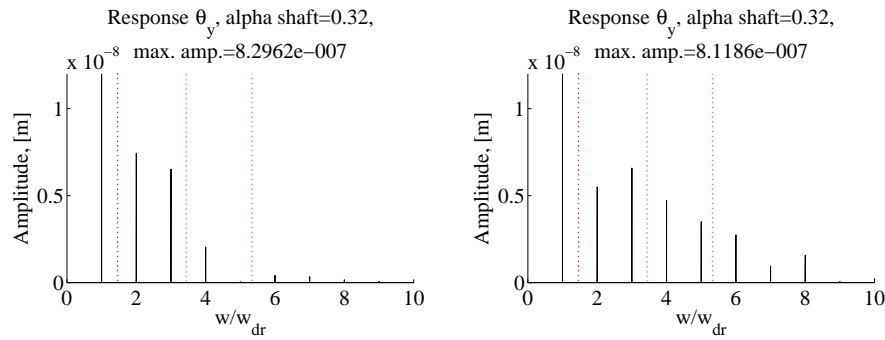


Figure 4.12: Response in θ_y , $\alpha = 0.32$. Black lines are the amplitudes of the response in the simulation, red lines are the eigenfrequencies of the system. (Left) mean shape deviation. (Right) two shape deviations.

4.3 Response to special case

A special case is studied where the mean shape deviation is set on the upper half of the generator, corresponds theoretically to asymmetric rotor, with large shape deviation on the upper part.

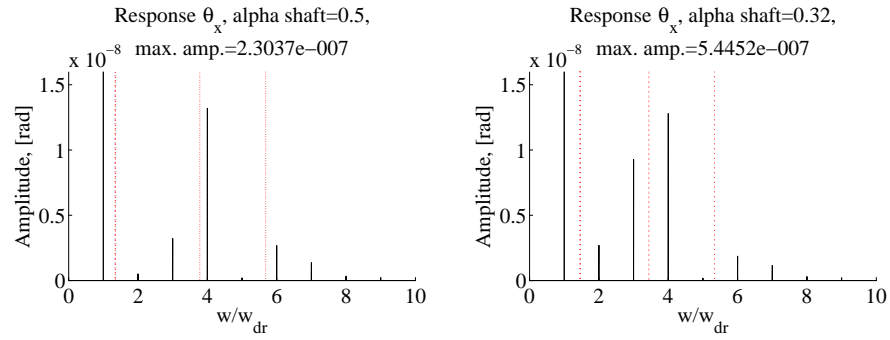


Figure 4.13: Response in θ_x for mean force set on the upper half of the generator. Black lines are the amplitudes of the response in the simulation, red lines are the eigenfrequencies of the system.

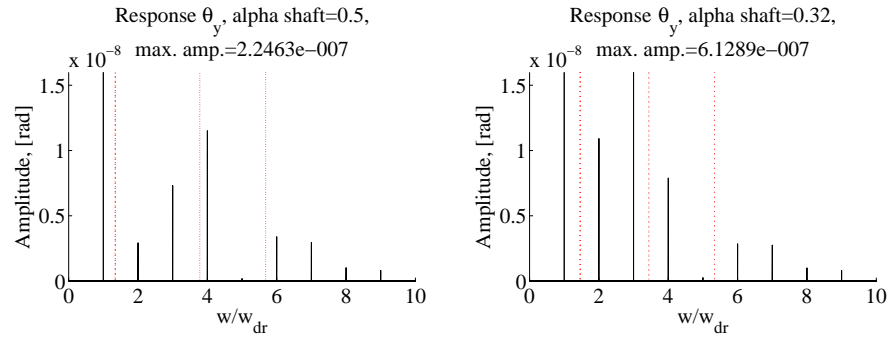


Figure 4.14: Response in θ_y for mean force set on the upper half of the generator. Black lines are the amplitudes of the response in the simulation, red lines are the eigenfrequencies of the system.

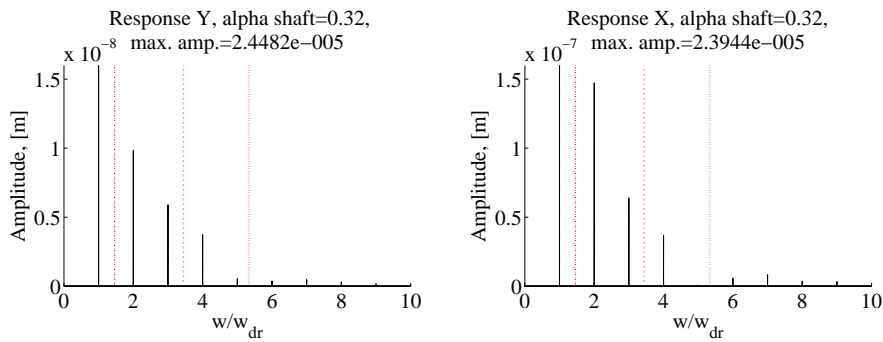


Figure 4.15: Response in X for mean force set on the upper half of the generator. Black lines are the amplitudes of the response in the simulation, red lines are the eigenfrequencies of the system.

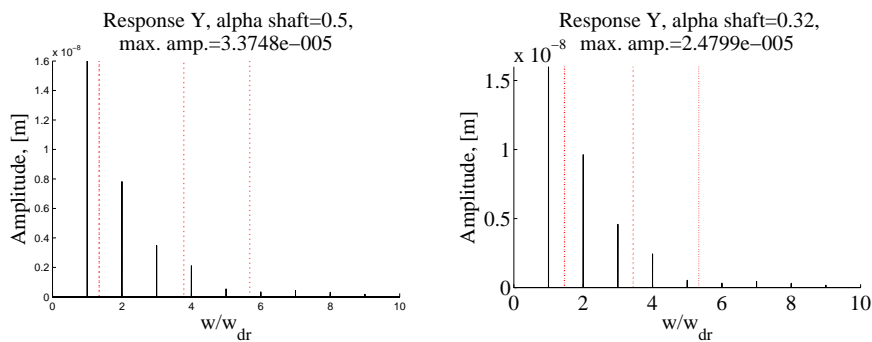


Figure 4.16: Response in Y for mean force set on the upper half of the generator. Black lines are the amplitudes of the response in the simulation, red lines are the eigenfrequencies of the system.

Chapter 5

Discussion

In this thesis the rotor system is modeled as a mass-less shaft, bearings are assumed to be linear and the generator is assumed to be rigid. The electromagnetic force is modeled as a linear displacement dependent force with only a radial component. The model is used to predict response due to two shape deviations.

The values of the shape deviations were given from a SARA(Stator, Shaft, Rotor, Analysis) report of Krångfors G2, where upper and lower shape on the rotor and stator have been measured. The measurements were made on the upper and lower edge of the generator. The mean shape deviation is calculated from the upper and lower measurements. Because only two measurements have been made on the Krångfors G2, one on the upper edge and one on the lower edge of the generator, it doesn't give a good picture of the shape of the rotor and stator. It is not certain that the mean shape deviation can be approximated to the center of the rotor from the two measurements, the case might be that it actually will have a levering arm due the asymmetry in the shape of the rotor. Therefore three cases have been studied, mean shape deviation on the center of the generator, two shape deviation one on the upper half and one on the lower half of the generator and the mean shape deviation on only the upper half of the generator.

Figure 4.1 and 4.2 show that there is no difference in the forces when comparing the mean shape deviation with two shape deviations. This can also be seen in Equation (2.38) and (2.39) compared to Equation (2.40) and (2.41) where the top two terms are equal but the bottom two differ. The difference is seen in Figure 4.3 and 4.4, as bending moments in new frequencies.

The effect of the bending moments are seen in Figure 4.9, 4.10, 4.11 and 4.12, there is a clear difference in the amplitude of the different frequencies of the response. For a centered rotor $\alpha = 0.50$ there exists a bending moment for the case of two shape deviation but none for the case with a mean shape deviation. For the case $\alpha = 0.32$ there exists bending moments for both cases, but frequency spectrum differs. Especially higher frequencies don't appear in the mean shape case, but exist in the case of two shape deviations.

The main interest for this thesis has been to compare the difference of using two measured shape deviations for rotor and stator compared to the use of the mean value of these two measurements. It has been seen that the effect on the displacement in the x and y directions were small from two shape deviations. The two shape deviations resulted instead in a bending moment

in new frequencies that did not exist in the case with a mean shape deviation. This bending moment affected the angular displacement of the rotor around the x and y axes. For the case Krångfors G2 the angular displacement was very small, due to it being a very stiff system. Some of these frequencies were close to eigenfrequencies of the system, which could lead to increased excitation of a weaker system.

Also a special case was studied, the mean shape deviation was set on the top half of the rotor and the bottom half of the rotor was set to have no shape deviation. This case was studied to see the effects of an asymmetric rotor with large shape deviations on only a part of it. Figure 4.13 and 4.16 show the frequency spectrum for the response. It is seen that the response is larger in some frequencies than for the case of two shape deviations.

5.1 Conclusions

One can conclude

- Two shape deviations have small effect on the displacement of the rotor in X and Y directions.
- Two shape deviations give rise to bending moments in new frequencies, these bending moments give rise to displacements in θ_x and θ_y . In Krångfors G2 only the first frequency of the shape deviation can possibly affect the system.
- A mean shape deviation only on the upper part of the generator has larger effects in some frequencies than two shape deviations. This is due to that the moments that cancel partly in the case of two shape deviations, will be added together in the case of a mean shape deviation on the upper part. The conclusion is that two shape deviations can have a stabilizing effect compared to a large shape deviation on one part of the generator and none on the other.

Bibliography

- [1] International Hydro Power Association, International Commission on Large Dams, Implementing Agreement on Hydropower and Canadian Hydropower association, (2000): *Hydropower and the World's Energy Future; The role of hydropower in bringing clean, renewable, energy to the world.* Downloaded from <http://www.ieahydro.org/reports/Hydrofut.pdf>
- [2] Swedish Energy Agency, *Vattenkraften i Sverige, en faktarapport inom IVA-projektet energiframsy Sverige i Europa*, [http://www.energimyndigheten.se/web/biblshop.nsf/FilAtkomst/VattkIVA.pdf/\\$FILE/VattkIVA.pdf?OpenElement](http://www.energimyndigheten.se/web/biblshop.nsf/FilAtkomst/VattkIVA.pdf/$FILE/VattkIVA.pdf?OpenElement)
- [3] Rankine, W.J.M. 1869. *On the centrifugal force of rotating Shafts*, Engineer, Vol. 27, 249-249.
- [4] Jeffcott, H. H. 1919. *The lateral vibration of loaded shafts in the neighborhood of a whirling speed* Phil. Mag., Vol, No 1, 50-65.
- [5] Stodala, A. 1924. *Dampf- und Gas-Turbinen*, Verlag von Julius Springer.
- [6] Green, P. 1948. *Gyroskopisk effects of the critical speeds of flecible rotors.* Journal of Applied Mechanics, No 15, 369-375
- [7] Toshio, Y., Ishida, Y. 2001 *Linear And Nonlinear Rotordynamics* Wiley-Intersciences, New York. ISBN 0-471-18175-7
- [8] Gray, A., Pertsch, JR, G. 1918. *Critical Review of the bibliography on inbalanced magnetic pull in dynamoelectric machines.*
- [9] Belmans, R., Geysen, W. Jordan, H. Vandeput, A. *Unbalance Magnetic Pull and Homopolar Flux in Three Phase Induction Motors with Eccentric Rotors.* Proceedings, International Conference on Electrical Machines-Design and Application, Budapest, 916-921, 1982.
- [10] Arkkio, A., Antila, M. Pokki, K. Simon, A. Lantto, E. *Electromagnetic force on a whirling cage rotor*, IEE Proce.-Electr. Power Appl., Vol. 147, No5. September 2000.
- [11] Guo, D., Chu, F., Chen, D. 2001. *The Unbalanced Magnetic Pull and its effects on vibration in a three-phase generator with eccentric rotor.* Juornal of Sound and Vibration (2002) 254(2), p 297-312.

- [12] Wang, Y., Sun, G., Huang L. *Magnetic Field-induced Nonlinear Vibration of an Unbalanced Rotor*. ASME, Design Engineering Division (Publication) DE, v 116, n 2, Proceedings of the ASME Design Engineering Division - 2003 Volume 2, 2003, p 925-930.
- [13] Gustavsson, R., Aidanpää J-O. 2004. *The influence of magnetic pull on the stability of generator rotors*. ISROMAC- 10th International Symposium on Rotating Machinery. Honolulu, Hawaii, USA 2004. ISSN 1402-1757
- [14] Karlsson, M., Aidanpää J-O. 2006 *Dynamic behaviour in a hydro power rotor system due to the influence of generator shape and fluid dynamics*. Proceedings of PWR2005 ASME Power April 5-7, 2005, Illinois.
- [15] Lundstrom, N. 2006 *Dynamic Consequences of Shape Deviations in Hydro-power Generators*. Licentiate Thesis Luleå University of Technology. ISSN 1402-1757
- [16] Lundstrom, L., Gustavsson, R., Aidanpää, J-O. Dahlbäck, N., Leijon, M. 2005 *Influence on the stability of generator rotors due to radial and tangential magnetic pull force*. IET Electric Power Applications. January 2007. Volume 1, Issue 1, p. 1-8.
- [17] Karlsson, M. 2006 *Electro-Mechanical Modelling and Analysis of Hydroelectric Rotor Systems*. Licentiate Thesis Luleå University of Technology. ISSN 1402-1757
- [18] Genta, G. 1999. *Vibration of structures and machines, 3rd ed*. Springer, New York. ISBN 0-387-98506-9
- [19] Kreyszig, E. 1999. *Advanced engineering mathematics*. John Wiley and Sons, Inc. New York.